Presented at the Topical Conference on
Baryon Resonances, Oxford, England,
July 6 - 9, 1976

LBL-5502

NEW DATA ON $K^- p \to \bar{K}^0 n$ AND A $\bar{K}N$ PARTIAL WAVE ANALYSIS BELOW 1.2 GeV/c

Robert D. Tripp

July 1976

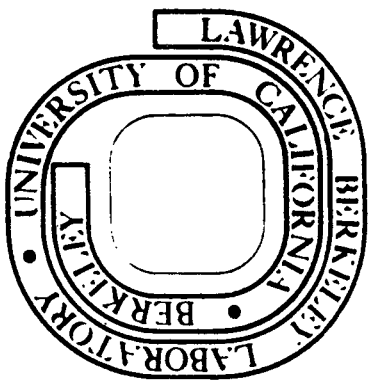

Prepared for the U. S. Energy Research and
Development Administration under Contract W-7405-ENG-48

DISCLAIMER

NEW DATA ON $K^- p \to \bar{K}^0 n$ AND A $\bar{K}N$ PARTIAL WAVE ANALYSIS BELOW 1.2 GeV/c

Robert D. Tripp

Department of Physics and
Lawrence Berkeley Laboratory
Berkeley, CA 94720

1. Introduction

I shall report on a preliminary partial wave analysis of $K^- p$ elastic and charge-exchange scattering. The justification for yet another such analysis derives from the fact that we have recently completed a precision measurement of the charge-exchange total cross section from 515 to 1066 MeV/c from which we would like to draw conclusions concerning Y*'s in this mass region. We are also preparing data from a charge-exchange angular distribution experiment which we intend eventually to incorporate into this partial wave analysis.

The experiment, a joint venture of LBL (Alston-Garnjost, Kenney, Pollard, Ross, Tripp), Mt. Holyoke (Nicholson), and CERN (Ferro-Luzzi), is a counter experiment done at BNL in which the charge-exchange total cross section is measured at 48 momenta (almost every 10 MeV/c) with a statistical precision of better than 1%. The existing bubble chamber data are shown in Figure 1 along with some predictions from earlier analyses while our new data appear in Figure 2. Agreement between the two figures in both cross section and momentum is quite good, although our results show some significant structural differences. The deep U-shaped valley at $\Lambda\eta$ threshold (725 MeV/c) is now clearly delineated, being more steep-sided and flat-bottomed than would be suggested from the bubble chamber data. This, we believe, is a manifestation of the S01 resonance and cusp at $\Lambda\eta$ threshold in combination with new evidence of a narrow P11 resonance near 750 MeV/c. Above that there is a shoulder more evident than in the bubble chamber data with a suggestion of a slight dip at $\Sigma^0\eta$ threshold (888 MeV/c). Finally the peak at 1050 MeV/c coming from the dominant F05 resonance is slightly lower in our data than is indicated from bubble chamber results. The apparatus used in the experiment, shown in Figure 3, differs only slightly from that employed to measure the $\bar{p}p \to \bar{n}n$ cross section and is adequately described in Ref. 1.

2. Parametrization

The basic partial wave analysis program is an outgrowth of the CHS analysis program.[2] We have incorporated into it a number of important sophistications deemed necessary for the elastic amplitudes in this energy region. First, we have imposed on the parametrization single-channel unitarity in the conventional way by multiplying the background S matrix element by the resonant S matrix element. Thus, $S = S_B S_R$ leading to a scattering amplitude $T = T_B + S_B T_R$. Resonant amplitudes are parametrized as Breit Wigner resonances with barrier factors (of the Glashow-Rosenfeld type) appropriate to the angular momentum state. For S wave resonances we have introduced cusps at $\Lambda\eta$ and $\Sigma^0\eta$ thresholds by adding a partial width for these processes to the total width in the amplitude denominator: $\Gamma_T = \Gamma_o + \gamma\, p$. Here p is the momentum of the η in the cm (imaginary below threshold) and $\gamma_\Lambda = .1$ and $\gamma_\Sigma = .3$ are adjusted to give the observed threshold enhancements in the $\Lambda\eta$[3] and $\Sigma^0\eta$[4] channels. Γ_o, the total width without the η channel, is a parameter of the fit. Finally the background amplitude in each partial wave has been made explicitly unitarity-conserving by parametrizing it in terms of a variable scattering length, viz. $T_B = \beta A/(1-i\beta A)$. Here β is a centrifugal barrier factor (G-R type) appropriate to the partial wave and $A = a + ib^2$ is the momentum-dependent complex scattering length. Thus,

$$a = \sum_{n=0}^{\leq 2} a_n P_n(x) \quad \text{and} \quad b = \sum_{n=0}^{\leq 2} b_n P_n(x) \quad \text{where}$$

$P_n(x)$ are Legendre polynomials and the argument x is proportional to the momentum, $-1 \leq x \leq +1$, spanning the fitted momentum interval. We square b so that the imaginary part always remains positive. For S and P waves n = 0, 1, and 2, was generally found necessary while for D and F waves n = 0 was adequate. The latter backgrounds were thus parametrized by a constant scattering length, whereas S and P wave backgrounds assume a more flexible behavior while retaining the unitarity-conserving feature.

3. Data

The fit, extending from 365 to 1200 MeV/c, uses the high statistics data of K-65[5] at the low momentum end to fix the amplitudes in the region of Λ (1520). Table I shows the data used. Items 2 (Yale), 3, and 5 are new data and have not been incorporated into previous analyses. Preliminary BNL results on total cross sections were interpolated to momenta where other types of data existed. Their isospin-decomposed total cross sections were assigned a 3% uncertainty whereas other cross sections were introduced with their quoted statistical error. 1271 data points were used in the fit. χ^2/data point = 1.49 for the best current fit.

4. Results

Preliminary results for the resonant amplitudes are listed in Table II. Figures 4, 5 and 6 show the Argand diagrams for the S and P wave amplitudes. Here we combine in each diagram the I = 0 and 1 amplitudes to facilitate visualizing their effect on the charge-exchange cross section since the charge-exchange amplitude is just the difference, $T_{\bar{K}^o n} = (T_1 - T_0)/2$; the integrated cross section involves no interference between various partial waves

$$\sigma_{\bar{K}^o n} = 4\pi \lambda^2 \left[|T_S|^2 + |T_{P1}|^2 + \ldots\right] .$$

The effects of the cusps are apparent in Figure 4. To see this, recall that the amplitude moves along its trajectory with a speed approaching infinity below and above the cusp, making the requisite 90° left-hand turn in passing through the cusp from below. Thus the S-wave charge-exchange amplitude, being impelled by the narrow S01 resonance just above Λη threshold, can be seen to diminish rapidly as it approaches the Λη cusp from below. Then as the I = 0 amplitude makes a left-hand turn at the cusp, $T_1 - T_o$ remains constant above. This leads to the rapid fall and flat-bottomed cross section as observed in Figure 2. Similar arguments explain the less pronounced behavior near Ση threshold. We find that the I = 0 S-wave amplitude is best represented by a broad resonance at higher energy overlapping the well-established resonance near Λη threshold. The I = 1 amplitude seems best fit by a broader resonance just above Ση threshold with a width consistent with that found in the Ση channel.[4]

The P01 amplitude seen in Figure 5 has a surprisingly narrow resonance on top of a large background presently parametrized as non-resonant but which may possibly be better represented as a broad resonance. This narrow effect needs further study as to its origin in the data. P11 has a broader but still narrow resonance at 1677 MeV, apparently a result of the rapid rise in the charge exchange cross section about the Λη cusp. At this early stage these are all the non well-established resonances we see although the broad structures in P11 and P03 may eventually be better described by resonances than by backgrounds. Our amplitudes, in general, agree well with those of the RL-IC analysis[14] although the data selection and parametrizations are quite different. We find no evidence for a resonance in our charge-exchange cross sections between 500-600 Mev/c where the BNL σ_1 cross section has substantial structure. A resonance here would be consistent with our lack of structure only if it were in a higher partial wave (for example D13 as suggested by Litchfield[15]).

A few types of data and their fits are shown in Figures 7, 8 and 9. As seen in Figure 7 all of our structure in the charge exchange cross section is followed rather well by the fit, yet the χ^2 is too high. This may reflect some additional uncertainties not included in the small statistical errors on the data points. For example, we may eventually have to fine-tune the momentum scale since our 0.5% momentum uncertainty is not small compared to cusp effects. With the addition of our precise charge-exchange data, the elastic channel suffers. Figure 8 shows the elastic cross section. As with previous partial wave analyses, we seem to be missing some important structure in the vicinity of 800 MeV/c. Figure 9 also shows the K^-p A1 coefficient to be underestimated at lower momenta. These are the only serious discrepancies that appear between the data and the fit. We are in the process of adding some recently published electronic data[16] on K^-p elastic scattering to strengthen this channel in the overall chi-squared fitting.

TABLE I

	DATA TYPE	DATA POINTS	SOURCE	MOMENTUM (MeV/c)
1.	$\frac{d\sigma}{d\Omega}$ K^-p, $\bar{K}^0n$	629	K-65 (5)	365-425
			CHS,CH (6)	436-1200
			Ch-LBL (7)	862-1001
			RL-IC (8)	960-1200
2.	Polarization K^-p	388	CERN-Holland (9)	862-1174
			Yale (Preliminary (10)	650-1087
3.	σ $\bar{K}^0n$	48	LBL (11)	515-1066
4.	$\sigma_T,\sigma_0,\sigma_1$	127	BNL (Preliminary) (12)	436-1200
5.	α_{K^-p}, α_{K^-n}	79	CERN-Caen (13)	436-1200

TABLE II

L,I,2J	MASS(Mev)	WIDTH(Mev)	ELASTICITY
SO1	1669	34	.2
	1728	142	.3
S11	1782	91	.25
PO1	1817	12	.1
P11	1677	25	.12
PO3	[1900]	[72]	.1
P13			
DO3	1519	15	.44
	1697	58	.22
D13	1682	71	.1
DO5	[1825]	[90]	.02
D15	1779	128	.36
FO5	1821	81	.60

In addition F15(1936), F17(2030) and G07(2100) are introduced as fixed resonances.

REFERENCES

This work was done with support from the U.S. Energy Research and Development Administration.

1. M. Alston-Garnjost et al., Phys. Rev. Lett. 35, 1685 (1975).
2. R. Armenteros et al., Nucl. Phys. B14, 91 (1969), Hemingway et al., Nucl. Phys. B91, 12 (1975).
3. D. Berley et al., Phys. Rev. Lett. 15, 641 (1965).
4. M. Jones, Nucl. Phys. B73, 141 (1974).
5. T. Mast et al., LBL 4294 and Phys. Rev. D (in press).
6. R. Armenteros et al., Nucl. Phys. B21, 15 (1970), B. Conforto et al., Nucl. Phys. B34, 41 (1971).
7. M. Jones et al., Nucl. Phys. B90, 349 (1975).
8. B. Conforto et al., RL 75-098.
9. S. Andersson-Almehed et al., Nucl. Phys. B21, 515 (1970) and M. Albrow et al., Nucl. Phys. B29, 413 (1971).
10. M. Zeller (private communication).
11. M. Alston-Garnjost et al. (to be published).
12. K. Li (private communication).
13. P. Baillon et al., Phys. Lett. 61B, 171 (1976) and Nucl. Phys. B107, 189 (1976).
14. G. Gopal et al., RL 75-182.
15. P. Litchfield, Phys. Lett. 51B, 509 (1974).
16. C. Adams et al., Nucl. Phys. B96, 54 (1975).

FIGURE CAPTIONS

Figure 1. Previous measurements of the $K^- p \to \bar{K}^0 n$ total cross section along with fits to the data by three partial wave analyses.

Figure 2. Preliminary results of our counter experiment to measure the charge-exchange cross section.

Figure 3. Apparatus used to measure the charge-exchange cross section.

Figure 4. Trajectories of the I=1 and I=0 S-wave amplitudes as a function of K^- lab momentum. The charge-exchange S-wave amplitude is given by $(T_1 - T_0)/2$.

Figure 5. Same as fig. 4 but for the P1 amplitudes.

Figure 6. Same as fig. 4 but for the P3 amplitudes.

Figure 7. Our $\bar{K}N$ fit to the charge exchange cross section.

Figure 8. The $K^- p$ total elastic cross section measurements along with our $\bar{K}N$ fit.

Figure 9. The A1 coefficient in the $K^- p$ angular distribution along with our $\bar{K}N$ fit.

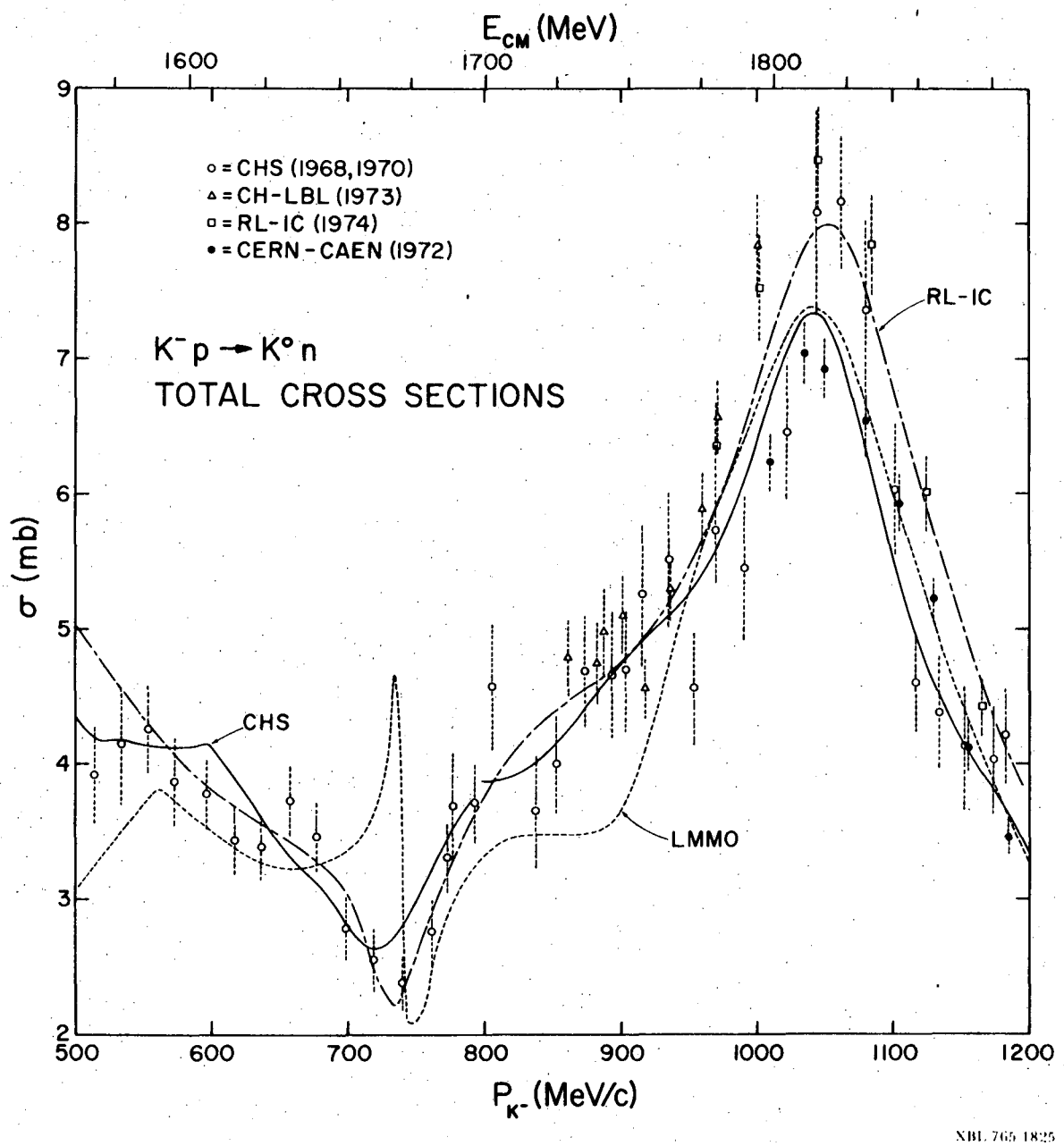

Fig. 1

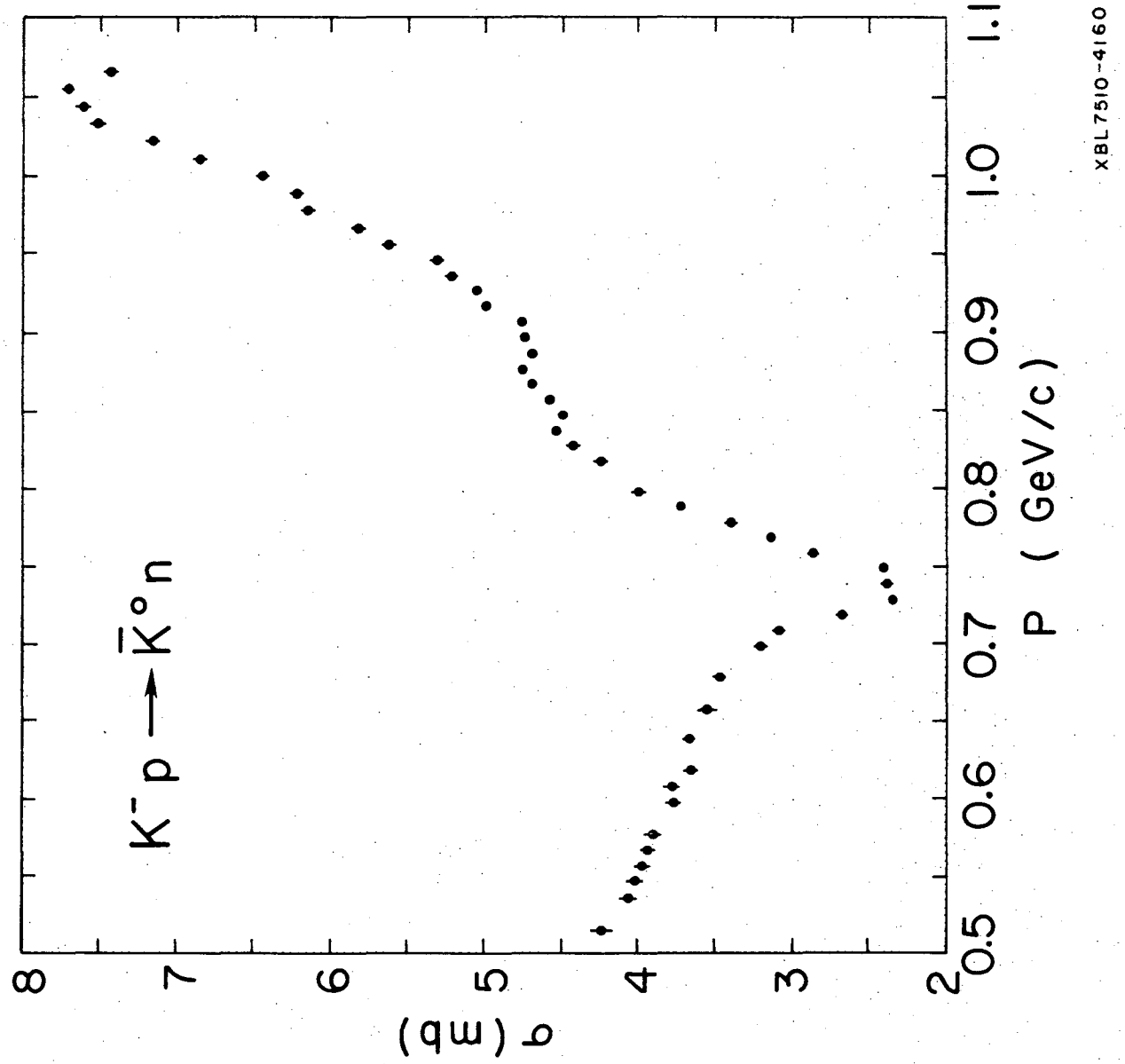

XBL7510-4160

Fig. 2

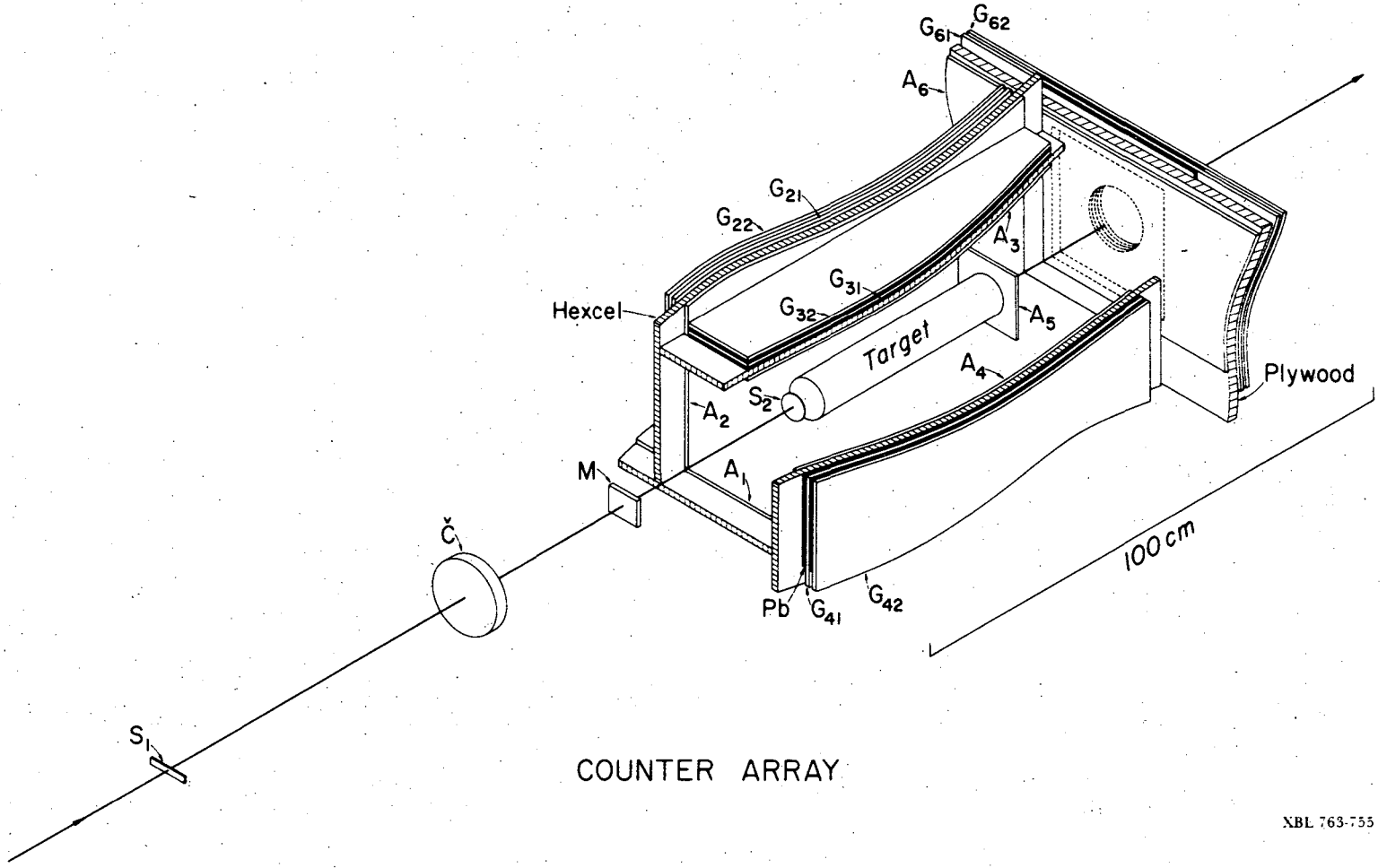

COUNTER ARRAY

XBL 763-755

Fig. 3

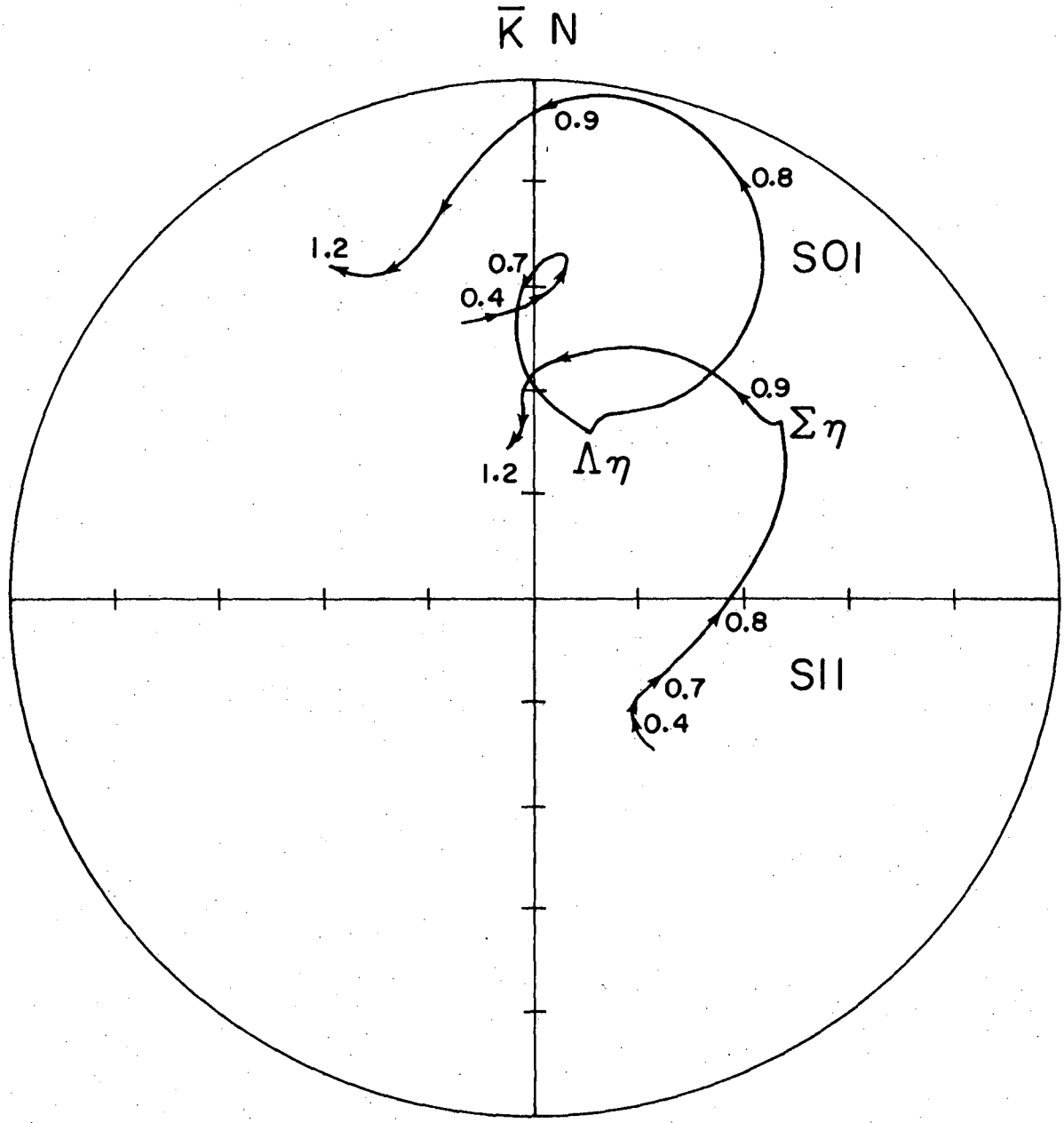

XBL 767-3110

Fig. 4

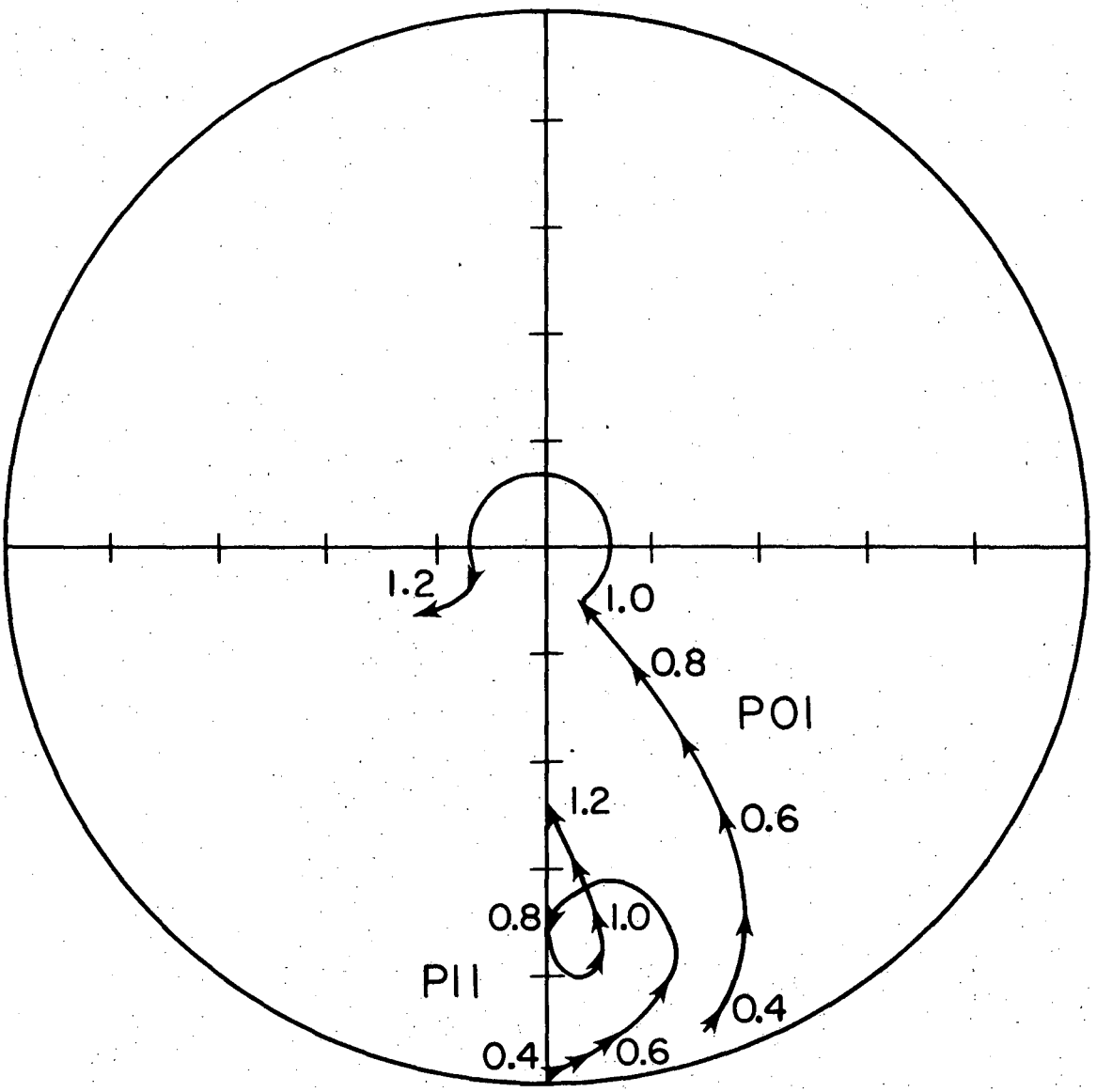

Fig. 5

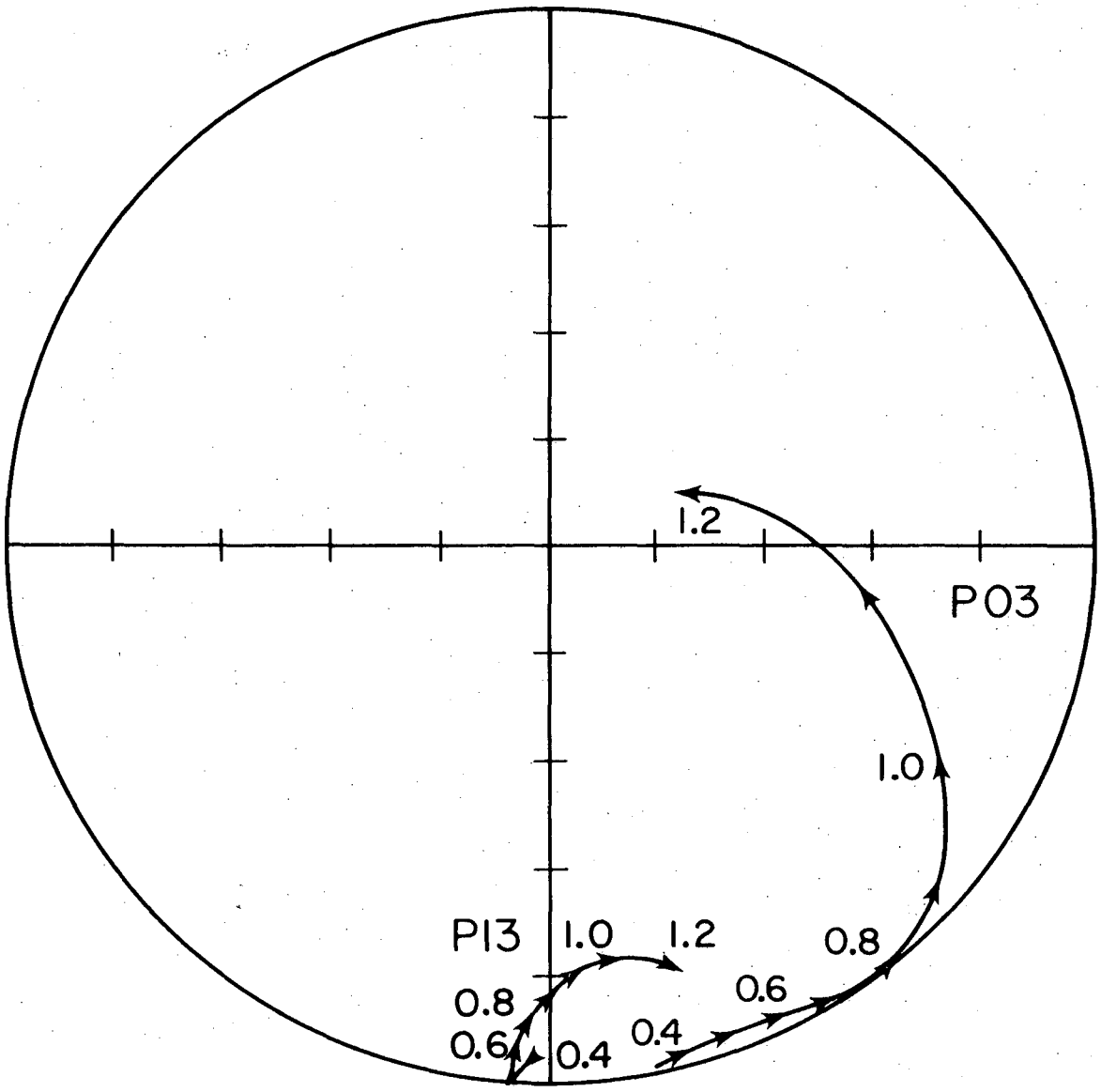

XBL 768-3325

Fig. 6

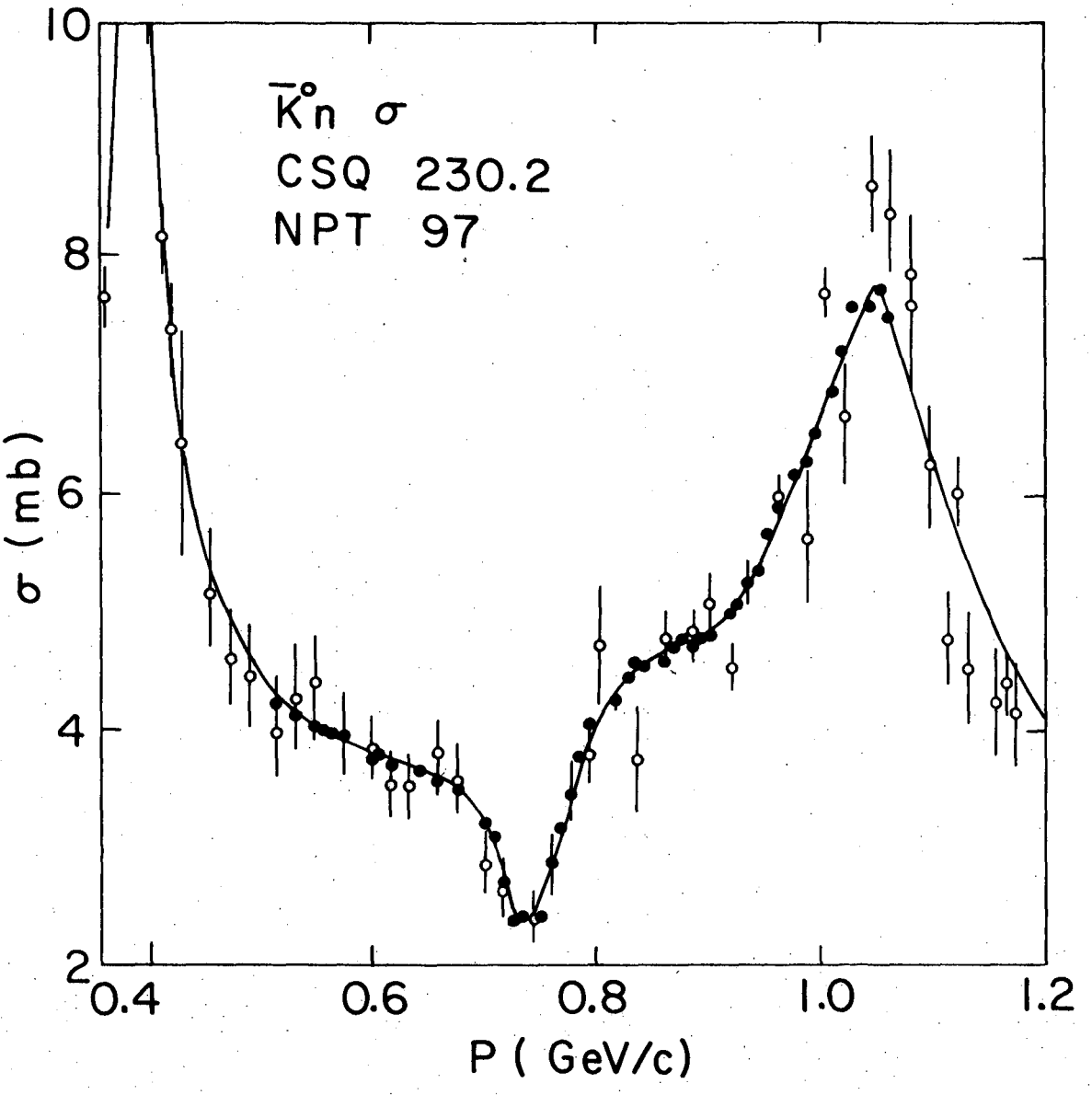
$\bar{K}^0 n$ σ
CSQ 230.2
NPT 97
σ (mb)
P (GeV/c)
10
8
6
4
2
0.4
0.6
0.8
1.0
1.2
XBL768-3350

Fig. 7

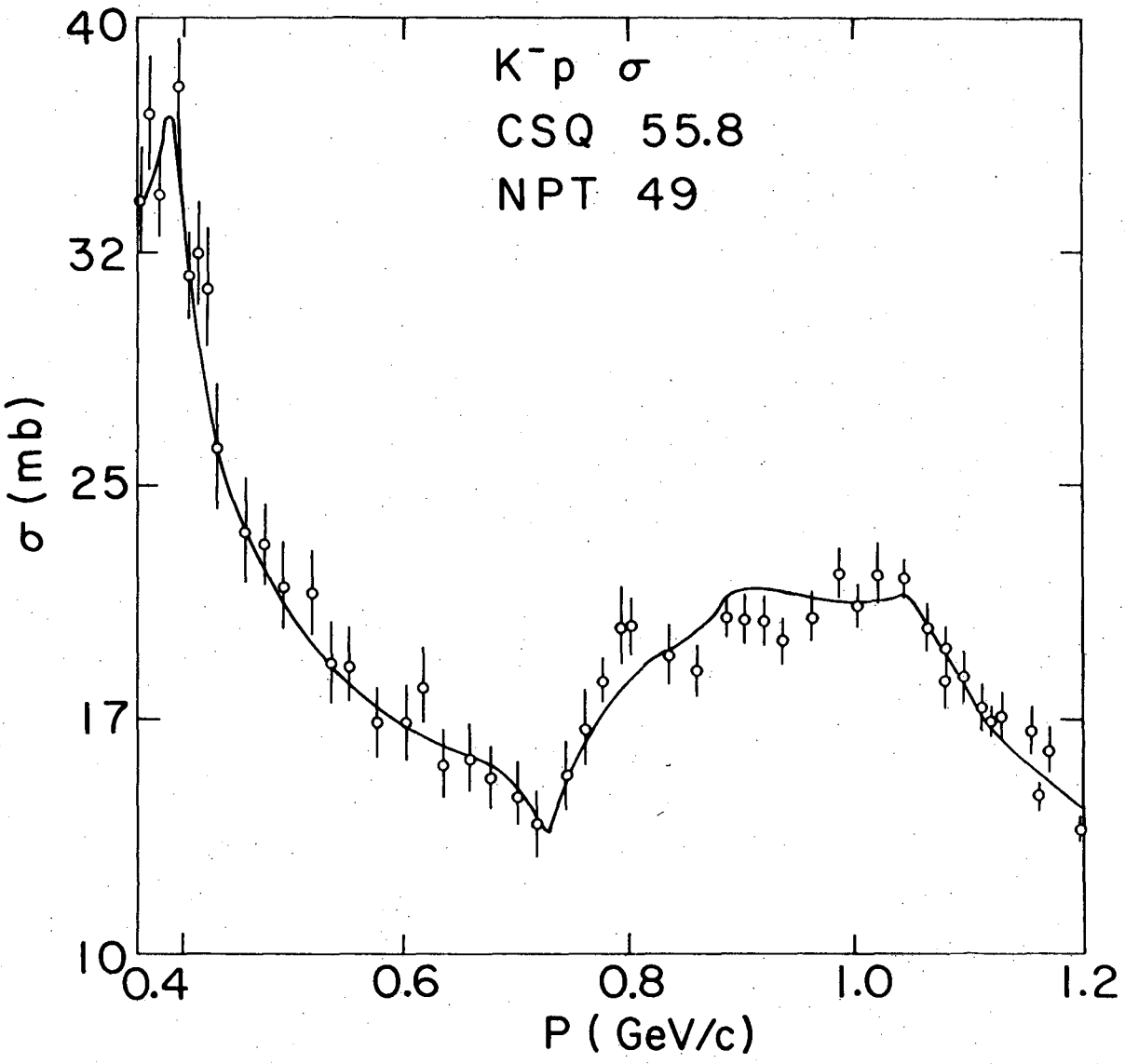
K⁻p σ
CSQ 55.8
NPT 49
σ (mb)
40
32
25
17
10
0.4
0.6
0.8
1.0
1.2
P (GeV/c)
XBL768-3349

Fig. 8

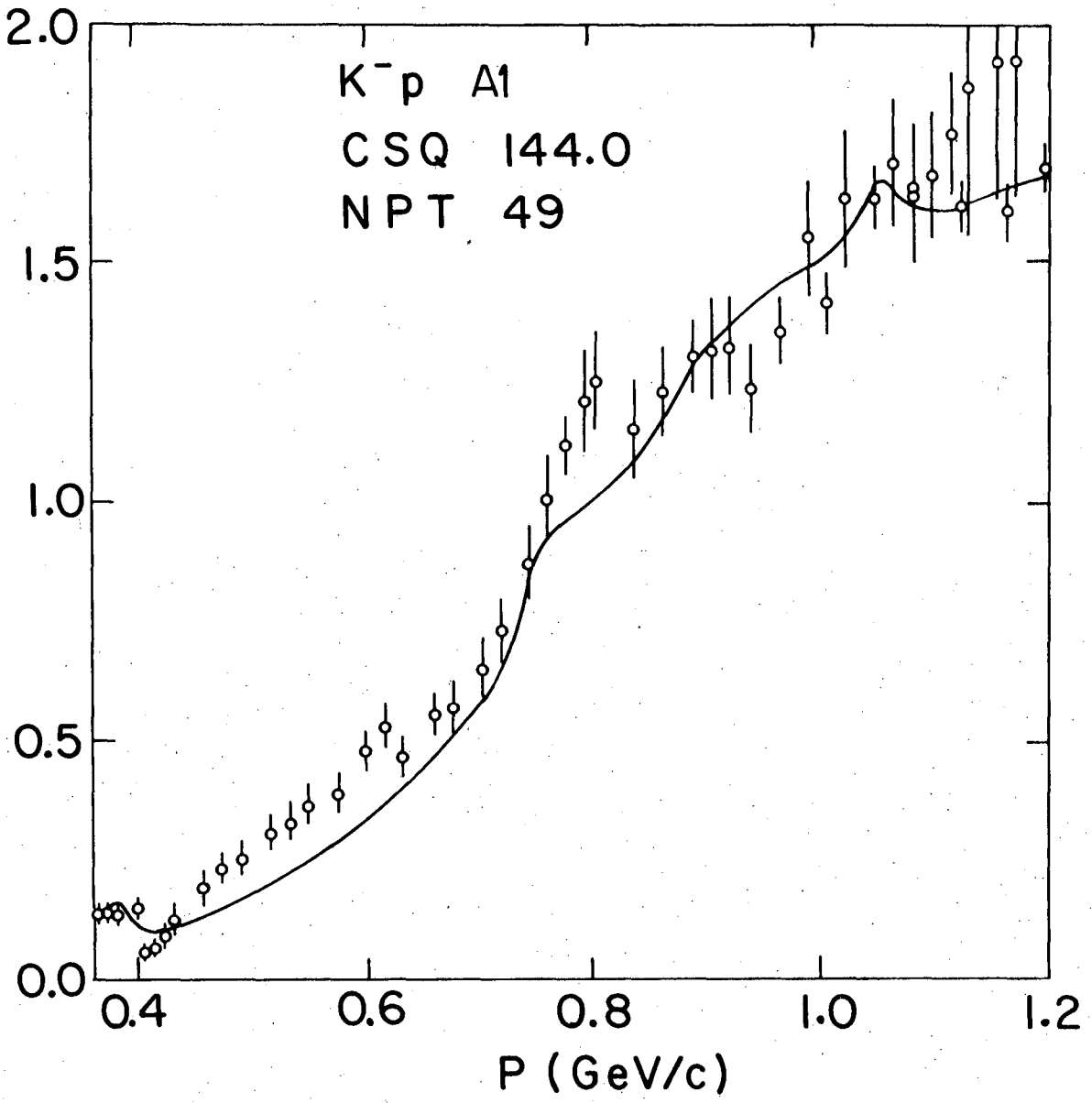

XBL768-3351

Fig. 9

TECHNICAL INFORMATION DIVISION
LAWRENCE BERKELEY LABORATORY
UNIVERSITY OF CALIFORNIA
BERKELEY, CALIFORNIA 94720